Electronic and Vibrational Structure of Copper Dibromide

Martin Lorenz and Vladimir E. Bondybey*

Institute for Physical and Theoretical Chemistry, Technical University of Munich, Lichtenbergstrasse 4, 85747 Garching, Germany

Received: December 7, 2001; In Final Form: February 28, 2002

Absorption and laser-induced fluorescence spectra of copper dibromide in a solid neon matrix are reported. Similar to those for copper dichloride, electronic transitions between the low-lying so-called ligand field states states are forbidden by the u↔g rule, appear as a result of vibronic Herzberg−Teller coupling. The observed transition energies are in good agreement with the adiabatic state energies derived from a recent gas-phase photodetachment study by Wang and co-workers. The matrix study with its much higher resolution yields detailed information about the copper halide electronic states and their vibrational structures.

Introduction

Despite the deceptively simple electronic structure of ground-state Cu atoms, with a closed d electron shell and a single 4s electron, copper exhibits complex redox chemistry for a transition metal. Both monovalent and divalent compounds of copper are common, and the Cu(I)/Cu(II) oxidation plays an important role in numerous biological processes.[1−3] Higher oxidation states of copper are also known and appear to be important in high-temperature superconductors.[4] A number of years ago, a visible spectrum observed in low-temperature matrices[5] and initially believed to be due to diatomic CuO was shown to be actually due to an interesting linear and centrosymmetric copper dioxide, OCuO, with a formally tetravalent copper atom.[6−8] This result was subsequently confirmed both by observing the linear isomer in the gas phase by photodetachment experiments from the corresponding anion[9] as well as by deriving its properties by computational techniques.[10]

Although copper monohalides were studied fairly extensively,[11−14] much less is known about the corresponding dihalides.[15−20] Notwithstanding the $3d^{10}4s\ ^2S$ Cu ground state of the copper atom, the ground states of molecular dihalides can be viewed as ionic, so-called "ligand-field" $X^-\ Cu^{2+}X^-$ states, formally arising from a $d^9\ Cu^{2+}$ core whose degeneracy is split by the field of the negatively charged chloride ligands.[15] High-quality theoretical relativistic ab initio calculations of Bauschlicher and Roos have predicted $^2\Pi_g$ ground states for the halides and gave the energies and ordering of the low-lying states,[20] but for a long time, there was no experimental verification. Besides the $X\ ^2\Pi_g$ ground state, the ligand-field splitting should also yield low-lying $^2\Sigma_g^+$ and $^2\Delta_g$ states. An absorption from the $X^2\Pi_g$ state to a higher-lying $^2\Pi_u$ state near 15 500 cm^{-1} is the most extensively studied transition of the dichloride. The excited so-called charge transfer state can be viewed as a superposition of the XCu^+X^- and X^-Cu^+X ionic structures and arises formally from binding between an ionic $d^{10}\ Cu^+$ core with two halogens.[15,20]

Several years ago, we investigated the halogen halides in rare gas matrices and showed that detailed information about their low-lying states can be obtained.[21,22] Although all the ligand-field states are of gerade symmetry and electronic transitions between them are forbidden, we have shown that an interesting vibronic Herzberg−Teller coupling[23] makes them weakly allowed. Excitation of the visible charge transfer is followed by an efficient nonradiative relaxation that populates the lower-lying ligand-field states, and extensive fluorescence between these states can then be observed.

Very recently, Wang and co-workers have reported elegant photodetachment experiments on the $CuCl_2^-$ and $CuBr_2^-$ anions.[24] These yielded information about the electron affinities and energies of the individual electronic states of the neutral copper dihalides, but their vibrational structure was not resolved. The appearance of these gas-phase results has now motivated us to report our solid neon matrix results for copper dibromide as well. The matrix data yield not only more accurate energies of the low-lying electronic states but also extensive information about their vibrational structure. They also provide interesting insights into the vibronic coupling, which makes the appearance of the forbidden transitions in the matrix possible. In this paper, we therefore report the spectra of copper dibromide in solid neon and compare the results with the gas-phase data and theoretical results, and we compile and tabulate the available information about copper dihalides.

Experimental Section

The copper dibromide fluorescence spectra were first observed[25] in our laboratory with the help of a self-igniting pulsed discharge technique[26] employing a dilute mixture of $CFBr_3$ with neon (1:400) and copper electrodes. When the discharge products were trapped at 5 K, the samples exhibited a structured absorption spectrum with an origin near 11 500 cm^{-1}. Excitation of this absorption by a Ti−sapphire laser produced strong near-infrared fluorescence beginning slightly below 8700 cm^{-1}. The same spectrum could also be produced using elemental bromine instead of $CFBr_3$, with the subsequent analysis suggesting that the emitter is the triatomic copper dibromide, $CuBr_2$.

In most of the experiments reported here, the pulsed laser vaporization technique was used.[27,28] The matrix-isolated bromide could be produced either by vaporizing a copper target in the presence of a neon carrier gas doped with bromine or by direct vaporization of copper dibromide. The $CuBr_2$ powder was pressed into a 13-mm diameter, 2-mm thick disk, which was then vaporized by frequency-doubled Nd:YAG laser pulses (3

* Corresponding author. E-mail: bondybey@uci.edu.

10.1021/jp014441w CCC: $22.00
Published on Web 05/14/2002

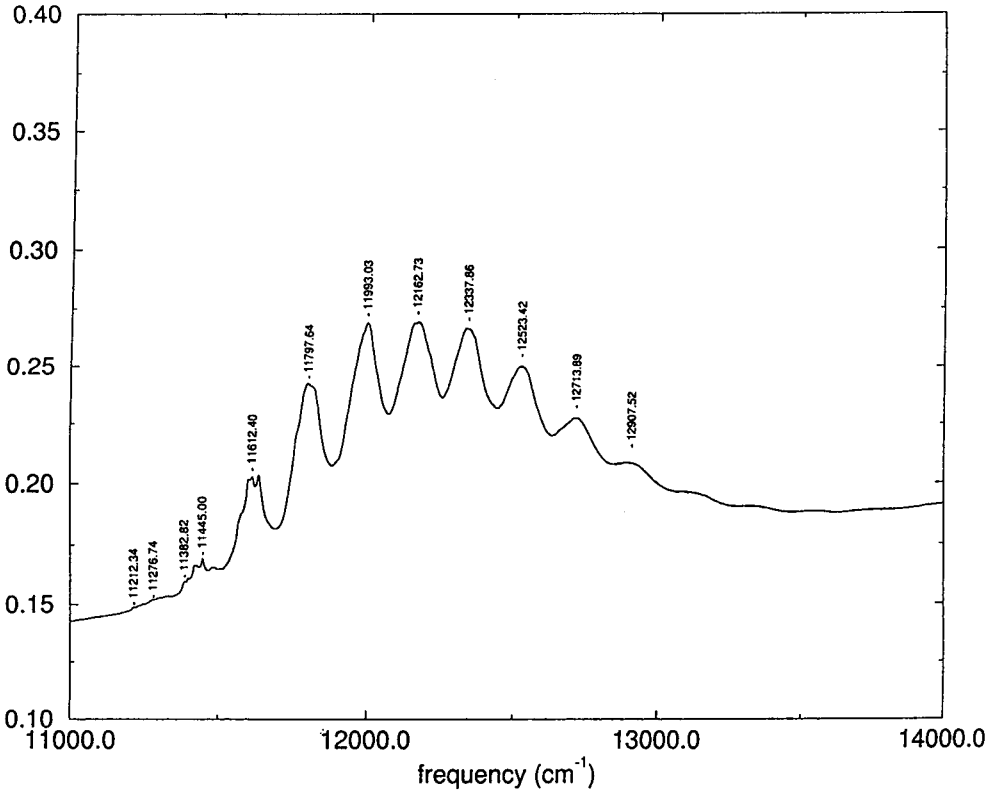

Figure 1. Near-infrared $E^2\Pi_u-X^2\Pi_g$ absorption spectrum of laser-vaporized copper dibromide isolated in solid neon at about 7 K. Note the hint of fine structure for the lowest-energy bands.

mJ, 10 ns). The laser pulses were synchronized with the opening of a pulsed piezoelectric valve controlling the carrier gas flow. The vaporization products swept by the gas pulse expanded into the vacuum of the cryostat and were deposited onto a silver-plated copper substrate cooled to ~6 K by a Leybold RGD 580 closed cycle refrigerator. Typically, the pellet was ablated at a 10 Hz repetition rate for 1−2 h using a neon backing pressure of 5 bar.

The absorption and fluorescence spectra were measured on a Bruker IFS 120-HR Fourier transform spectrometer. The absorption was measured in the range of 600−30 000 cm^{-1} with a resolution of 1 cm^{-1} or better. For the fluorescence experiments, the samples were excited by an argon laser-pumped tunable CW dye laser or a Ti−sapphire laser. Depending on the spectral range of interest, either a photomultiplier or a liquid nitrogen-cooled germanium or indium antimonide detector was used.

To facilitate the interpretation of the spectra, we have carried out a series of computations on a Pentium III-based Linux system using the Gaussian 95 suite of programs. For most of the computations, we have employed the hybrid B3LYP method as implemented there, using the pseudorelativistic effective core basis set of the Stuttgart−Dresden group (SDD).[29,30] Specifically relevant to the present work are the vibrational stretching fundamentals of $\nu_1 = 201$ and $\nu_3 = 376$. The ground $X^2\Pi_g$ state of the linear, open-shell $CuBr_2$ is subject to Renner−Teller splitting, and quantum mechanical computations yield two different values in place of the doubly degenerate bending mode. As will be shown, the components of the nominal $^2\Pi_g$ state are widely separated because of large spin−orbit coupling in the heavy $CuBr_2$ molecule, and the vibrational structure we observe provides no evidence of the Renner−Teller effect. In discussing the results, we will use a bending frequency of $\nu_2 = 65$ cm^{-1}, which is the average of the two computed values, 82 and 48 cm^{-1}.

Results and Discussion

Near-Infrared Absorption Spectrum. As noted above, matrices containing copper halides can be generated by several different methods: by laser vaporization of copper in the presence of a carrier gas doped with small amounts of the halogen, by electric discharge through a dilute Br_2− or Cl_2−Ne mixture using copper metal electrodes, or by direct laser vaporization of the solid copper halide. The results are relatively independent of the method used; in each case, one obtains rather intense near-infrared absorptions due to the copper II halides.

As shown in Figure 1, in the case of $CuBr_2$, the absorption spectrum starts around 11 212.34 cm^{-1} and consists of an extended but rather irregular progression of broad bands with an approximately 180 cm^{-1} spacing. The individual absorption bands have different shapes, and some (in particular, the ones at the low-energy end) seem to exhibit fine structure. When one tries to fit the measured absorption maxima to a single progression, a vibrational frequency of about 180 cm^{-1} is obtained, but the fit is poor and the positions of individual bands show appreciable random deviations from the computed positions. On the basis of the absorption intensities, the transition involved must be quite strong and probably fully allowed, but when it is excited by a laser tuned to the region of absorption, there seems to be very little or no resonant fluorescence back into the ground state, suggesting that the excited state preferentially relaxes nonradiatively.

On the other hand, when an infrared detector is used, strong fluorescence that starts at a much lower energy (below 9000 cm^{-1}) is observed, which leaves an appreciable gap between the origins of the absorption and emission spectra. By modulating the laser source and using lock-in detection of this infrared fluorescence while scanning the laser frequency in the region of the absorption origin, one obtains the excitation spectrum shown in Figure 2. This spectrum clearly parallels the structured

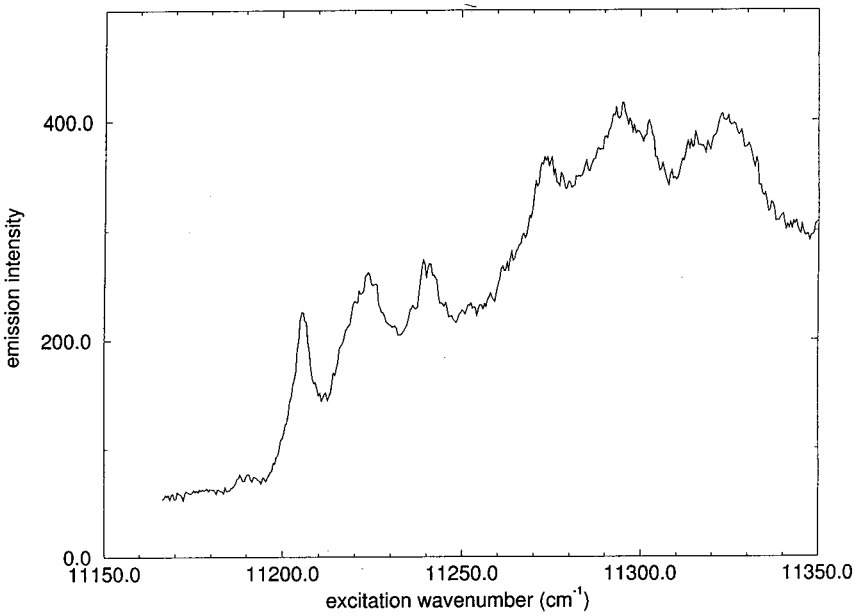

Figure 2. Excitation (yield) spectrum of $CuBr_2$ near the $E^2\Pi_u-X^2\Pi_g$ origin. It was obtained by monitoring the overall intensity of the near-infrared fluorescence and scanning the Ti−sapphire laser in the region of the lowest-energy bands of Figure 1.

absorption, proving that the emission is due to the same carrier that is responsible for the near-infrared absorption spectrum. As will be discussed below, a detailed analysis of the fluorescence spectrum unambiguously identifies this carrier as linear, centrosymmetric copper dibromide, $CuBr_2$. The excitation spectrum, compared with the direct absorption, exhibits a considerably improved resolution and signal-to-noise ratio. It shows that the lowest energy absorption bands exhibit a reproducible sharp structure, which is at least partially due to site effects, and reveals that the origin of the major site absorption is located at 11212.3 ± 0.1 cm^{-1}.

Laser-Induced Fluorescence Spectrum. When the laser excites the strong, broader bands near the intensity maximum of the absorption spectrum, the emission bands are relatively broad and seem to be doubled. This "doubled" appearance can be shown to be due to nonselective, simultaneous excitation of $CuBr_2$ trapped in several trapping sites. When, on the other hand, the laser is tuned to one of the weak maxima in the sharp structure near the absorption origin, the emission lines sharpen considerably and the band doubling disappears, which then greatly facilitates the analysis of the spectrum. As is usually the case with molecules of this type in matrices, $CuBr_2$ is trapped in solid neon in several sites that can be selectively excited by the laser. The one responsible for the 11 212.3 cm^{-1} origin gives rise to the most intense spectrum, with another slightly less intense site being shifted 27.4 cm^{-1} to lower energies. This "red" site exhibits, except for the uniform 27.4 cm^{-1} shift of all vibronic bands, spectroscopy and molecular constants identical to those of the more intense "blue" site on which the following discussion will now concentrate.

Selective excitation of the blue site results in a relatively sharp, well-resolved fluorescence spectrum, which is presented in Figure 3. Its overall intensity is suggestive of a vibrationally relaxed emission from the $v = 0$ level of some excited electronic state. The spectrum extends from an origin in the neighborhood of 8700 cm^{-1} to well beyond the ∼7000 cm^{-1} cutoff of the germanium detector. Note that the intensity scale in the second panel of Figure 3 is expanded by about a factor of 10. The most intense "main" bands in the spectrum form a regular, nearly harmonic progression starting with a strong, sharp line at 8689.0 ± 0.1 cm^{-1} followed by a series of bands with an ∼226 cm^{-1} spacing. This spacing is appropriate for assignment to a Cu−Br stretching frequency but clearly too high to be attributed to a bending frequency of a triatomic molecule like $CuBr_2$. In bent molecules, usually the bending angle is the parameter that is most sensitive to electronic excitation, resulting in prominent progressions in the bending frequency in the electronic spectrum. This result suggests that if the spectrum is attributed to $CuBr_2$, the molecule should be linear, similar to the $CuCl_2$ and CuF_2 species.

Although the first band of the main progression at 6870 cm^{-1} (denoted 0,1 in Figure 3) is relatively sharp, the lower-energy, higher members of the progression broaden, and starting with the third (2,1 in Figure 3) band, they show signs of a triplet structure. This structure becomes much better resolved in the following bands of the progression, with the bands denoted 4,1, 5,1, and 6,1 being clearly resolved triplets with approximate intensity ratios of about 1:2:1. This is what should be expected for the v_1 vibrational progression of a linear centrosymmetric $CuBr_2$ molecule, with the $^{79}BrCu^{79}Br$, $^{79}BrCu^{81}Br$, and $^{81}BrCu^{81}Br$ isotopomers in natural isotopic abundances. Although the presence of some of the weaker bands can be shown to be due to inhomogeneous "site effects" that are caused by imperfect site selection and incomplete suppression of the $CuBr_2$ molecules isolated in the spectrally shifted "sites", other bands cannot be explained in this way, and we will return to a more detailed analysis of the emission spectrum in a later section.

When an indium antimonide detector with a response extending further into the infrared is employed instead, a second, lower-energy spectrum extending between about 6900−6100 cm^{-1} is observed, as shown in Figure 4. Its structure appears relatively simple and similar to the higher-energy Ge detector region spectrum described above. It consists of a single progression of at least four rather strong bands with an origin at 6870 cm^{-1} and an ∼225 cm^{-1} spacing. As in the higher-energy spectrum, the first band at 6870 cm^{-1} is relatively sharp, but the higher members of the series progressively broaden and when examined more carefully, again suggest the triplet structure with about a 1:2:1 intensity ratio. This result is indicative of a linear−linear electronic transition of a centrosymmetric $CuBr_2$.

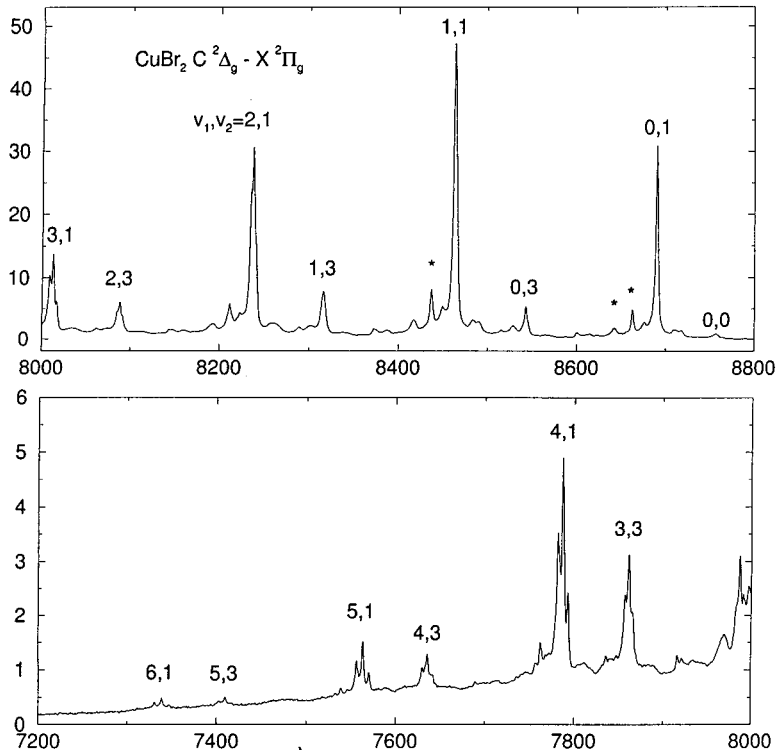

Figure 3. Infrared $C^2\Delta_g-X^2\Pi_g$ ($^3/_2$) emission spectrum of $CuBr_2$ excited at 11 382 cm^{-1}. The strongest progression starting with the false origin at 8689.7 cm^{-1} appears because of vibronic coupling with the π_u υ_2 promoting mode. Note the clearly resolved 1:2:1 triplets for the higher vibrational levels due to bromine isotopic splitting. The true origin at 8756 cm^{-1} appears weakly and is denoted by an arrow. Note the weak progressions involving the $3\upsilon_2$ and $5\upsilon_2$ levels. Bands marked by asterisks are due to $CuBr_2$ in a spectrally shifted site.

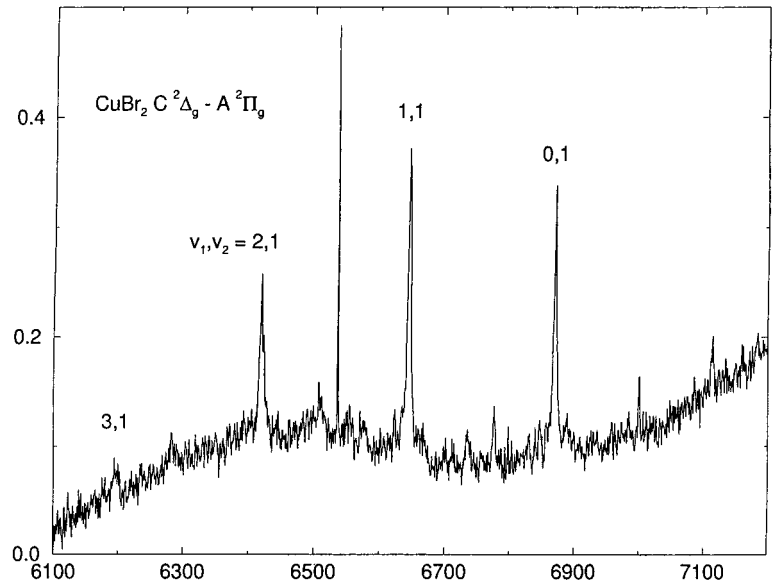

Figure 4. Lower-energy infrared fluorescence assigned to the $C^2\Delta_g-A^2\Pi_g$ ($^1/_2$) transition of $CuBr_2$ in solid neon at 7 K measured with an InSb detector. The sharp band at 6535.8 cm^{-1} is due to an unidentified impurity.

There may be at least three different interpretations explaining the fact that two separate band systems, presented in Figures 3 and 4, that are both due to the same $CuBr_2$ molecule are observed:

(a) The band systems represent emissions from two different fluorescing states, separated in energy by 1820 cm^{-1}, into the same lower state, presumably the $CuBr_2$ ground state.

(b) The band systems represent emissions from one fluorescing state into two lower-lying states, presumably the $CuBr_2$ ground state, and a low-lying excited state at about 1820 cm^{-1}.

(c) It is much less likely that two different emitting states as well as two different lower states are involved.

Possibility (a), involving the same lower state, can be easily eliminated because even though the lower states of the two transitions have very similar vibrational frequencies, detailed analysis reveals that these frequencies are well outside the experimental error. The spacings between the first and second bands of the main progressions are 226.48 and 225.04 cm^{-1} for the two transitions, which gives a difference of 1.44 cm^{-1} whereas the mean error of the entire fit of the spectrum of more than 30 observed isotopic bands[30] (to be described below) is $\sim$0.16 cm^{-1}. It seems, therefore, that possibility (b) must be preferred, that is, a nonradiative relaxation of the absorbing state at 11 212.3 cm^{-1} populates a single state at 8689.6 cm^{-1}, which

then fluoresces into the ground state as well as into a low-lying excited state some 1820 cm^{-1} higher in energy.

Electronic Structure of $CuBr_2$ and the Absorbing State. There is little experimental information about the triatomic copper dihalides; also, theoretical calculations for species of this type are difficult. The open d electron shell of transition metals still represents a considerable challenge, and for a molecule containing heavier halogen relativistic effects, it become increasingly important. Although copper dibromide was not extensively studied, about a decade ago Bauschlicher and Roos[20] carried out detailed computations for the lighter $CuCl_2$ and CuF_2 species, which we found a few years ago to be extremely useful in interpreting our experimental laser-induced fluorescence and absorption spectra of matrix-isolated copper dichloride.[21] Both the energies of the low-lying electronic states and their vibrational structures proved to be very consistent with the observed spectra. Also, the results of a recent low-resolution photodetachment study of $CuCl_2$ anions showed satisfactory agreement with the results of Bauschlicher and Roos.[20] Although their computations did not extend to the isovalent dibromide, in general its electronic structure can be expected to be quite similar.

The $CuBr_2$ ground state and its lowest excited state should again be the so-called ligand-field states arising formally from an ionic Cu^{2+} cation with two Br^- anions. Ligand-field theory shows that depending on the orientation of the hole in the d^9 core the degeneracy will be split, resulting in $^2\Sigma_g^+$, $^2\Pi_g$, and $^2\Delta_g$ electronic states, with ab initio computations predicting the $X^2\Pi_g$ to be the ground state. In the heavy halides, the fine-structure components of the latter two states should split far apart because of spin−orbit coupling. Obviously, because all these states are of gerade symmetry, transitions between them should be strictly forbidden. It is again expected that levels arising from a closed-shell $3d^{10}$ Cu^+ configuration will be slightly higher in energy. These levels are, perhaps somewhat inconsistently, called charge-transfer states Because they can be viewed as a superposition of the $BrCu^+Br^-$ and Br^-Cu^+Br structures, at least in a formal sense, there is less charge transfer than in the ligand-field states. The lowest of these states will be a $^2\Pi_u$ state, with a fully allowed transition into the ground state. It seems inevitable that the strong absorption we observe starting at 11 212 cm^{-1} must be assigned to this transition.

The photodetachment spectrum of the $CuBr_2^-$ anion, reported recently by Wang et al.,[24] is useful in discussing the $CuBr_2$ state assignments. The spectrum is reproduced in a vertical orientation on the right-hand side of Figure 5. The authors[24] assigned the two bands denoted in Figure 5 as E and F to the ($^1/_2$) and ($^3/_2$) spin−orbit components, respectively, of this $^2\Pi_u$ electronic state and report energies of 10 550 and 11 800 cm^{-1} for these states. The features observed in the photodetachment spectrum are, however, quite broad; furthermore, the bands assigned to different states exhibit different widths and shapes. Therefore, measuring the separations of the band maxima may not be the most reliable way of determining the state adiabatic energies.

We have attempted to reanalyze the photodetachment spectra of both $CuCl_2$ and $CuBr_2$ by an alternative method. We have first extrapolated the steeply rising portion of each observed photodetachment band to find an intercept with the baseline, as suggested by the dotted lines in Figure 5. We have then converted the separations between intercepts obtained in this way into the adiabatic state energies and have obtained considerably different values of about 11 500 ± 200 and 12 700 ± 200 cm^{-1} for the E and F states, respectively. The former value is in very good agreement with the matrix ~11 200 cm^{-1} value for the absorbing state, supporting its assignment to the lower spin−orbit component of the $^2\Pi_u$ electronic state.

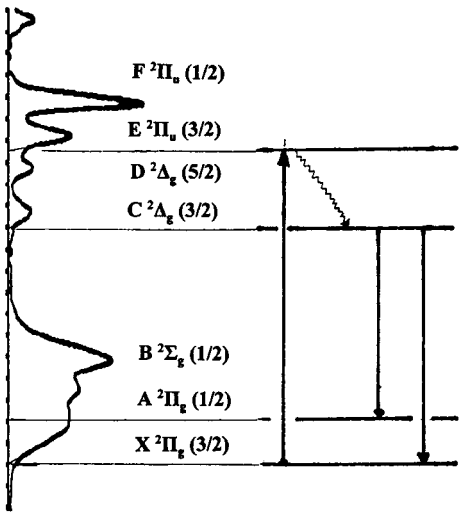

Figure 5. Energy levels of $CuBr_2$. The left-hand side shows a 193-nm photodetachment spectrum of $CuBr_2$ that was adapted from Figure 2 of ref 24. The upward-aiming arrow denotes the $E^2\Pi_u-X^2\Pi_g$ laser excitation. Following nonradiative relaxation of the E state (denoted by the wiggly arrow), probably via the $D^2\Delta_g$ state, emission is observed from $C^2\Delta_g$ into both the A and X components of the $^2\Pi_g$ ground electronic state.

Laser-Induced Fluorescence Spectrum and Identities of the States Involved. Because, as already noted and in contrast with $CuCl_2$,[22] no emission from the $E^2\Pi_u$ state back to the $X^2\Pi_g$ ground state is observed despite the fully allowed character of the transition, apparently $E^2\Pi_u$ must efficiently relax nonradiatively. The intense fluorescence starting more than 2000 cm^{-1} further into the infrared must then be assigned to emission from electronic states populated by this relaxation process. Because no states other than the ligand-field states discussed above are expected below the E state, it is clear that transitions between these states must be involved even though these are, as already mentioned, forbidden.

According to a standard treatment[23] that can be found in most physical chemistry textbooks, one writes for a transition moment between two electronic states

$$R_{ev} = \langle e',v''|\,\mu\,|\,e'',v''\rangle = \langle e'\,|\,\mu_e\,|\,e''\rangle\,\langle v'\,|\,v''\rangle = R_e\langle v'\,|\,v''\rangle$$

with the transition intensity being proportional to its square, R_{ev}^2. According to the Franck−Condon principle, the Born−Oppenheimer approximation allows a separation of vibrational and electronic motion and factoring of the electronic transition moment R_e. Here, the first factor, R_e, determines if the electronic transition is allowed, with the second and the Franck−Condon factors $\langle v'\,|v''\rangle^2$ determining the intensity distribution between various vibrational levels. For a given band to appear, the integrand in $\langle v'\,|v''\rangle$ has to be totally symmetric, and because most molecules are usually in the vibrationless level, only totally symmetric vibrations appear in the spectrum.

As realized by Herzberg and Teller,[23] the separation of the electronic and nuclear motion is not necessarily rigorous, and the dipole and the electronic transition moment R_e will change with the motion of the nuclei. To include this effect of vibronic coupling and the changes of the electronic transition moment with the motion of the nuclei, one can express the electronic transition moment in the form of a Taylor expansion in normal coordinates while retaining only the first two terms: $R_e \approx R_{e0} + \Sigma_i R_{ei}Q_i$ where $R_{ei} = \partial R_e/\partial Q_i$. Inserting this expression into

the above equation, one obtains

$$R_{ev} = \langle v' | \ R_e | v'' \rangle = R_{e0} \langle v' \mid v'' \rangle + \Sigma_i \, R_{ei} \langle v' \mid \ Q_i | v'' \rangle$$

Depending on the symmetry of the Q_i mode, the second term may be nonzero and result in nontotally symmetric vibrations appearing in the spectrum. Particularly interesting is the case where R_{e0} and the first term are zero, that is, the transition is forbidden, and only bands deriving their intensity from the second integral are observed. Transitions of this type are characterized by the absence of the true 0−0 origin and occurrence of progressions in the totally symmetric vibrations built upon "false origins" involving odd quanta of vibrations belonging to a symmetry species that makes the second integral nonzero. A typical example is the $A^1B_{2u}-X^1A_{1g}$ transition of benzene, where one observes in absorption as well as in emission progressions in the totally symmetric ν_1 vibration combined with 1 quantum of the e_{2g} ν_6 mode. A similar situation can also occur for copper dihalides, where the g−g electronic transitions are symmetry-forbidden but weak bands may appear because of vibronic interactions involving the ν_2 Π_u bending vibration.

As noted above, an analysis of the spectrum suggests that the fluorescence occurs from a state located at about 8700 cm^{-1} into the ground state and into a low-lying state at around 1800 cm^{-1}. In our recent study of $CuCl_2$, we have concluded[21] that the fluorescence originates from the lower component of the $^2\Delta_g$ ligand field, and a similar interpretation seems reasonable for the isovalent $CuBr_2$. The $CuBr_2^-$ photodetachment spectra of Wang et al.[24] exhibit two broad peaks in this region, which they label C and D. They assign them, by analogy to similar B and C peaks detected in the spectrum of the isovalent $CuCl_2$ molecule, to the two spin−orbit components of a $^2\Delta_g$ state and report values of 7650 and 9350 cm^{-1} for the vertical detachment energies of the $^2\Delta_g$ ($^5/_2$) and $^2\Delta_g$ ($^3/_2$) components, respectively. When we apply the same treatment we have used for the E state, that is, we find the photodetachment onset for each of the bands observed in the Wang et al.[24] spectrum, and then use these onsets rather than the band maxima of the broad bands to derive the adiabatic energies, we obtain values of 8700 and 10 500 cm^{-1} for the C and D states, respectively. The former value is again in satisfactory accord with the matrix observation.

The most consistent and reasonable interpretation of the neon matrix observations appears to be that the initially excited $E^2\Pi_u$ state relaxes nonradiatively into the slightly lower-lying $^2\Delta_g$ state and ends up in the vibrationless level of its lower component, the C state of Wang et al.[24] as shown schematically in the energy-level diagram presented on the right-hand side of Figure 5. This state then emits into the $^2\Pi_g$ ground state, with the higher-energy fluorescence in Figure 3 corresponding to the transition into the $X^2\Pi_g$ ($^3/_2$) ground state and the weaker emission in the InSb detector range (Figure 4) terminating in the higher $A^2\Pi_g$ ($^1/_2$) component. Table 1 gives a summary of the reported energies[24] of all the relevant states of $CuBr_2$ along with our revised values and compares them with the theoretical and neon matrix data.

Vibrational Structure of the $CuBr_2$ $^2\Pi_g$ Ground State. By accepting the interpretation that the symmetry forbidden transition occurs because of Herzberg−Teller vibronic coupling, the strongest bands have to be assigned to a progression of the type $1^0_n \, 2^0_1$, with the first band at 8689.6 cm^{-1} corresponding to the $n = 0$ false origin. This interpretation is then supported by the observation of a very weak "true" 0−0 origin at 8756.0 cm^{-1}, which is 66.4 cm^{-1} above the false one. Although in the gas phase this transition would be rigorously forbidden, it appears weakly because of interactions with the solid medium, yielding a value of 66.4 cm^{-1} for the "promoting" asymmetric π_u mode, in adequate agreement with theory. This result also explains the presence of another weaker progression originating at 8542.7 cm^{-1}, which is 146.9 cm^{-1} below the 8689.6 cm^{-1} band. This band is another false origin, with 3 quanta of the bending vibration, $3\nu_2'$ being the promoting level.

TABLE 1: Adiabatic Energies of the Low $CuBr_2$ Electronic States (cm^{-1})

	gas phase[a]	gas phase[b]	neon[c]	theory[d]
$X^2\Pi_g$ ($^3/_2$)	0	0	0	0
$A^2\Pi_g$ ($^1/_2$)	1050	1900	1820	
$B^2\Sigma_g^+$ ($^1/_2$)	2200	3100		1609
$C^2\Delta_g$ ($^3/_2$)	7650	8700	8756	7322
$D^2\Delta_g$ ($^5/_2$)	9350	10 500		
$E^2\Pi_u$	10 550	11 500	11 212	10 408
$F^2\Pi_u$	11 800	12 800		

[a] State energies as reported by Wang et al.[24] [b] Our values derived from our reevaluation of Wang et al.'s data[24] as explained in the text. [c] Neon matrix values from this work. [d] Theoretical results consisting of CCSD(T) calculations neglecting spin−orbit splitting.[24]

TABLE 2: Vibrational Constants of $^{63}Cu^{79}Br_2$ and $^{63}Cu^{35}Cl_2$ in Solid Neon (cm^{-1})

	T_0	ν_1	ν_2	$x_{1,1}$	$x_{2,2}$	$x_{1,2}$
			$CuBr_2$			
$X^2\Pi_g$ ($^3/_2$)	0	226.94	59.09	−0.24	2.37	0.63
$A^2\Pi_g$ ($^1/_2$)	1757.4	226.29		0.09		
			$CuCl_2$			
$X^2\Pi_g$ ($^3/_2$)	0	370.55	96.97	−0.52	4.48	−0.16
$A^2\Pi_g$ ($^1/_2$)	178	350.1	103.56	0.04	−0.38	

As noted above, the ν_1 progressions can be followed at least up to $\nu_1'' = 6$, with the higher members ($\nu_1'' \geq 3$) exhibiting a fully resolved bromine isotopic structure. The calculation of the isotopic factors ρ_i and the isotopic shifts in linear centrosymmetric molecules such as $CuBr_2$, where there is just one vibration of each symmetry species, is quite straightforward. In principle, bands involving the bending vibration should exhibit a $^{65}Cu-^{63}Cu$ isotopic structure, with $\rho_2(^{65}Cu) = 0.989$. Unfortunately, in view of the relatively large ~2 cm^{-1} line widths, the expected splitting of about 0.7 cm^{-1} is too small to be clearly resolved. The least-squares fit of all the observed bands using the appropriate isotopic relationships gives a mean-square deviation of 0.16 cm^{-1}. The bending ν_2 vibration exhibits a "negative anharmonicity", $x_{22} = 2.37$ cm^{-1}, which is reasonable because the bending potential must be symmetric and cannot contain cubic or higher-order odd terms. We list the vibrational constants of $^{63}Cu^{79}Br_2$ derived from the least-squares fits in Table 2, where they are compared with the corresponding values reported for $^{63}Cu^{35}Cl_2$.[21] Using the listed constants, the observed bands can be computed to within the experimental accuracy.

The second fluorescent transition observed with an origin at 6870 cm^{-1} is then again assigned to emission from the vibrationless level of the $C^2\Delta_g$ state into the higher spin−orbit component of the ground state, $A^2\Pi_g$. The emission is undoubtedly again due to vibronic coupling, but because the signal-to-noise ratio with the indium antimonide detector is considerably lower, neither the true origin nor the progression involving $3\nu_2''$ are observed in this case. The totally symmetric vibrational frequency is very similar to that in the lower component, but interestingly, although ν_1 of the higher state exhibits a small negative anharmonicity, that of the ground state has a regular anharmonicity. This result could be explained by interactions and "repulsion" between the two states in the matrix.

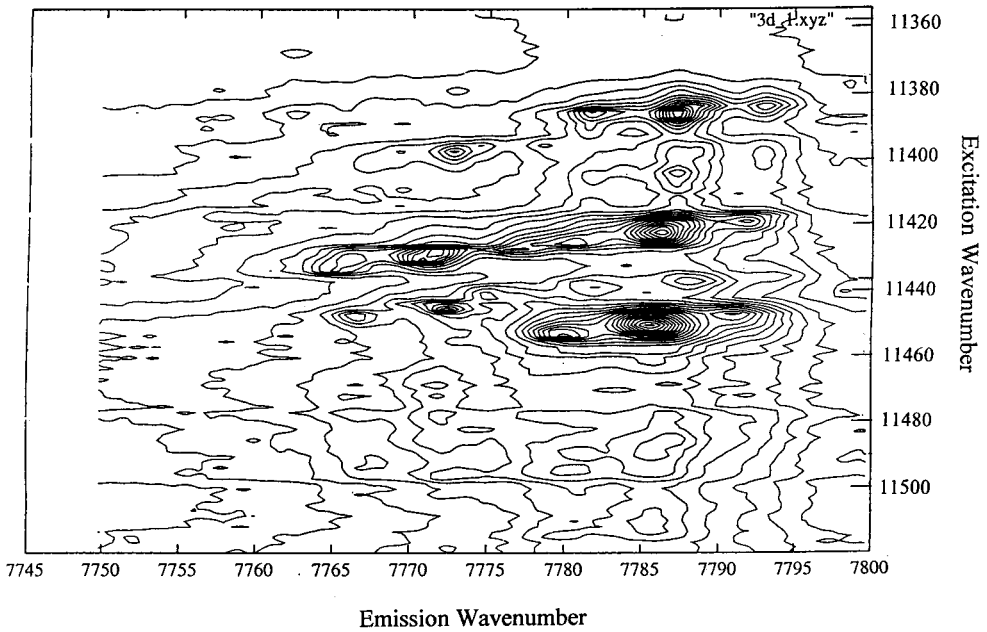

Figure 6. Three-dimensional equal intensity contour plot, with the excitation wavenumber on the ordinate and the emission wavenumber on the abscissa. Individual transitions appear as islands in this plot; different sites are diagonally shifted. Emission in the region of the $1^0_4 2^0_1$ transition is shown; note the horizontally clearly separated bromine isotopic triplets. The separation in the vertical direction is much smaller because the laser was scanned near the $v' = 1$ upper-state level.

The observed ground-state vibrational frequencies appear to be in acceptable agreement with our B3LYP density functional calculations as well as with the recent computational results of Wang et al.[24] The similar vibrational structure of the two states is consistent with their assignment to two components when one neglects the spin−orbit coupling of the same $^2\Pi_g$ ground state. Also, the 1820 cm^{-1} value does not appear unreasonable for the splitting of the two spin−orbit components in the heavy $CuBr_2$ molecule.

Site Effects and Matrix Shifts. It is often observed in matrices for both atoms and molecules that although transitions between states arising from the same electronic configuration appear sharp those involving configurational changes are broadened and exhibit larger inhomogeneous broadening and extensive phonon sidebands.[31] Also, in the present case, one can see by comparing the spectrum in Figure 1 with those in Figures 3 and 4 that although the bands due to the $C^2\Delta_g - A$, $X^2\Pi_g$ transitions between the ligand field states, which all formally arise from the d^9 Cu^{2+} configuration, appear sharp the interconfiguration $E^2\Pi_u - X^2\Pi_g$ bands (with the E state being derived from d^{10} Cu^+) are broad and the vibrational progression appears irregular. Usually, such interconfiguration transitions also exhibit much larger medium shifts from gas to matrix or from one matrix material to another.[31] Therefore, although the matrix values for the transitions between the different ligand field states should be within 1−2% of the free-molecule values, a somewhat larger medium shift might be expected for the $E^2\Pi_u - X^2\Pi_g$ spectrum.

The involvement of inhomogeneous broadening is clearly demonstrated by the laser excitation spectra and by the ability to excite individual sites selectively. In such cases, one can often get additional insight from 3-D plots where the emission wavenumber is on the abscissa, the excitation wavenumber is on the ordinate, and the lines connect points of equal emission intensity. Each vibronic transition appears in such a plot as a separate "island". Unfortunately, we could record such spectra only in a fairly narrow spectral region. Figure 6 displays a section of the emission around the $C^2\Delta_g - X^2\Pi_g$ $1_4^0 3_1^0$ band while the laser was tuned approximately to the $v'=1$ level of the $E^2\Pi_u$ state. One can clearly identify the Br_2 triplet near 11 387 cm^{-1} with the isotopic components separated horizontally by nearly 5 cm^{-1}, as expected for emission into the $v_1'' = 4$ level. The splitting in the vertical direction is much smaller (~1 cm^{-1}) because the $v_1' = 1$ level is excited. This triplet pattern is repeated ~35 and again ~64 cm^{-1} higher in energy. Some of these observations are clearly due to site effects, but in view of the limited excitation range available for study, the details of this structure are not fully understood.

The limited matrix data also does not provide any clear clues for the causes of the irregularity of the $E^2\Pi_u$ vibrational progression seen in Figure 1. The presence of Fermi resonances between the v_1 stretching vibration and the overtones of the v_2 bending vibration, resulting in unresolved "Fermi Polyads" could be one explanation. There is also no clear experimental proof that the charge-transfer upper state could not be bent, in which case progressions in the bending vibration could also be involved. Finally, interactions, perhaps matrix-induced, between the two E and F components of the $^2\Pi_u$ excited state could lead to irregularities in the vibrational structure. Clearly, a high-resolution gas-phase study would be helpful in providing a detailed understanding of the excited $E^2\Pi_u$ state properties.

Summary

Absorption and laser-induced fluorescence spectra of copper dibromide in solid neon were investigated. An absorption due to the $E^2\Pi_u - X^2\Pi_g$ transition with an origin near 11 212 cm^{-1} is observed. When the $E^2\Pi_u$ state arising from Cu^+ with the closed-shell d^{10} configuration is excited, it relaxes nonradiatively to lower-lying states, the so-called ligand field states of $CuBr_2$, which can be formally represented as a d^9 Cu^{2+} ion interacting with two bromide anions, and it populates the $C^2\Delta_g$ state. Two transitions from this state are observed in the emission that terminates in the $X^2\Pi_g$ ($^3/_2$) ground state and in the $A^2\Pi_g$ ($^1/_2$) spin−orbit component that is about 1820 cm^{-1} higher in energy. These symmetry-forbidden transitions are made possible by vibronic Herzberg−Teller coupling with the Π_u v_2 vibration

promoting mode. The bromine vibrational structure is clearly resolved, and a least-squares fitting of the observed bands yields the vibrational frequencies and anharmonicities of the states involved. The results for both $CuBr_2$ and $CuCl_2$ are tabulated and summarized and are compared both with theory and with the results of a recent gas-phase photodetachment study of the corresponding anions.

References and Notes

(1) Solomon, E. I.; Sundaram, U. M.; Machonkin T. E. *Chem. Rev.* **1996**, *96*, 2563.
(2) Cowan, J. A. *Inorganic Biochemistry: An Introduction*; VCH Publishers: New York, 1993.
(3) Tolman, W. B. *Acc. Chem. Res.* **1997**, *30*, 227.
(4) Bednorz, J. G.; Muller, K. A. *Z. Phys. B: Condens. Matter* **1986**, *64*, 189.
(5) Shirk, J. S.; Bass, A. M. *J. Chem. Phys.* **1970**, *52*, 1894.
(6) Tevault, D. E. *J. Chem. Phys.* **1982**, *76*, 2859.
(7) Bondybey, V. E.; English, J. H. *J. Phys. Chem.* **1984**, *88*, 2247.
(8) Caspary, N.; Savchenko, E. V.; Thoma, A.; Lammers, A.; Bondybey, V. E. *Low Temp. Phys.* **2000**, *26*, 744.
(9) Wu, H.; Desai, S. R.; Wang, L. S. *J. Phys. Chem. A* **1997**, *101*, 2103.
(10) Chertihin, G. V.; Andrews, L.; Charles, J.; Bauschlicher, C. W. *J. Phys. Chem. A* **1997**, *101*, 4026.
(11) Manson, E. L.; DeLucia, F. C.; Gordy, W. *J. Chem. Phys.* **1975**, *63*, 2724.
(12) Hikmet, I.; Dufour, C.; Pinchemel, B. *Chem. Phys.* **1993**, *172*, 147.
(13) Martin, T. P.; Schaber, H. *J. Chem. Phys.* **1980**, *73*, 3541.
(14) Winter, N. W.; Huestis, D. L. *Chem. Phys. Lett.* **1987**, *311*, 133.
(15) Leroi, G. E.; James, T. C.; Hougen, J. T.; Klemperer, W. *J. Chem. Phys.* **1962**, *36*, 2879.
(16) DeKock, C. W.; Gruen, D. M. *J. Chem. Phys.* **1968**, *49*, 4521.
(17) Roos, A. J.; Crozet, P.; Bacis, R.; Churassy, S.; Erba, B.; Ashworth, S. H.; Lakin, N.; Wickam, M. R.; Beattie, M. R.; Brown, J. M. *J. Mol. Spectrosc.* **1996**, *177*, 134.
(18) Bouvier, A. J.; Bosch, E.; Bouvier, A. *Chem. Phys.* **1996**, *202*, 139.
(19) Tokuda, T.; Fujii, N.; Yoshida, S.; Shimizu, K.; Tanaka, I. *Chem. Phys. Lett.* **1990**, *174*, 285.
(20) Bauschlicher, C. W.; Roos, B. O. *J. Chem. Phys.* **1989**, *91*, 4785.
(21) Lorenz, M.; Caspary, N.; Foeller, W.; Agreiter, J.; Smith, A. M.; Bondybey, V. E. *Mol. Phys.* **1997**, *91*, 483.
(22) Lorenz, M.; Smith, A. M.; Bondybey, V. E. *J. Chem. Phys.* **2001**, *115*, 8251.
(23) Herzberg, G. *Electronic Spectra of Polyatomic Molecules*; Kriegler Publishing Company: Florida, 1991.
(24) Wang, X. B.; Wang, L. S.; Brown, R.; Schwerdtfeger, P.; Schröder, D.; Schwarz, H. *J. Chem. Phys.* **2001**, *114*, 7388.
(25) Schlachta, R.; Lask, G.; Tsay, S. H.; Bondybey, V. E. *Chem. Phys.* **1991**, *155*, 267.
(26) Schlachta, R. Ph.D. Thesis, Technical University of Munich, Munich, Germany, 1993.
(27) Bondybey, V. E.; English, J. H. *J. Chem. Phys.* **1981**, *74*, 6978.
(28) Bondybey, V. E. *Science (Washington, D.C.)* **1985**, *227*, 125.
(29) Nicklass, M.; Dolg, M.; Stoll, H.; Preuss, H. *J. Chem. Phys.* **1995**, *102*, 8942.
(30) Lorenz, M. Ph.D. Thesis, Technical University of Munich, Munich, Germany, 2000.
(31) Rasanen, M.; Heimbrook, L. A.; Bondybey, V. E. *J. Mol. Spectrosc.* **1987**, *157*, 129.